Hindawi
International Journal of Photoenergy
Volume 2018, Article ID 8607247, 8 pages
https://doi.org/10.1155/2018/8607247

Research Article

Atmosphere-Dependent Photoconductivity of ZnO in the Urbach Tail

D. Scolfaro, Y. J. Onofre, M. D. Teodoro, and M. P. F. de Godoy

Departamento de Física, Universidade Federal de São Carlos (UFSCar), PA 167, São Carlos, SP 13565-905, Brazil

Correspondence should be addressed to M. P. F. de Godoy; mgodoy@ufscar.br

Received 12 July 2018; Revised 3 September 2018; Accepted 12 September 2018; Published 21 October 2018

Academic Editor: Yanfa Yan

Photoconductivity is a fundamental and highly applicable phenomenon for semiconductor oxide-based devices, and the presence of defects plays a significant role in this mechanism. Here, we present an investigation based on different atmospheres and light excitation (above and below bandgap) dependences of zinc oxide thin film grown by spray-pyrolysis. As-grown ZnO presents a representative Urbach tail associated to the presence of localized levels in the bandgap. Photoconductivity response and decay times are investigated for air and inert atmospheres as well as under vacuum conditions with significant features due to light excitation conditions. The observed characteristics are explained based on oxygen photodesorption when excitation is above bandgap while this process is suppressed when excitation is below bandgap.

1. Introduction

Wide bandgap oxide-based semiconductors are strategical materials for high-power electronics, transparent electrodes, and chemical gas sensors. Zinc oxide is a representative semiconductor which presents high transparency, direct bandgap, large exciton energy, and low toxicity. In a practical point of view, a great advantage is that ZnO can be produced in thin film form by several methods as rf-sputtering [1], pulsed-laser deposition (PLD) [2], chemical vapour deposition (CVD) [3], molecular beam epitaxy (MBE) [4], and spray-pyrolysis [5], which allows the fabrication of commercial electrical-electronic devices. As a semiconductor, the effect of photoconductivity is mainly explored using light sources in wavelengths which energies are higher than the bandgap and, for ZnO, it corresponds to the ultraviolet optical range (~3.3 eV). Despite being an intuitive phenomenon, which the absorption of a photon generates an electron-hole pair in conduction and valence bands, respectively, the photoconductivity depends strongly on surface properties, such as molecule adsorption and desorption processes as well as the presence of intrinsic defect levels near electronic bands which act to trap or detrap photocarriers. Consequently, the presence of some defects levels produces anomalous effects as persistent photoconductivity [6] and negative photoconductivity [7].

Nevertheless, these effects can be used to enhance gas sensing response using light excitation (even at room temperature) [8] and photocatalysis [9] as well as novel applications are considered with the utilization of persistent photoconductivity for holographic memories [10]. These mechanisms can also be explored in optical excitations below the bandgap [11]. Therefore, the transient response of photoexcitation plays a fundamental role for these applications.

However, the presence of defects in oxide semiconductors is strongly dependent on synthesis method. In the technological field of thin films, sophisticated techniques like MBE, PLD, or CVD [2–4] produce epitaxial films in appropriated substrates like sapphire with low defect levels. The low rate growth allows better crystalline conformation which can be evaluated by structural and electronic characterizations. The crystallinity of epitaxial films provides a near perfect crystal, but the maintenance of stoichiometry is still a challenge. At higher deposition rates, sputtering also provides suitable thin films, mainly polycrystalline, which the management of stoichiometry can be achieved by atmosphere control including oxygen [12, 13]. Alternative

techniques like sol-gel associated to dip-coating and spray pyrolysis can also be employed to thin film production avoiding the requirement of vacuum control and also producing polycrystalline films. In the case of defect-assisted phenomena, like optical absorption below bandgap, the management of growth conditions in a nonperfect method can play a significant role and avoids impurities doping. Among many techniques, the spray pyrolysis presents the advantage of low-cost implementation and the possibility of large area deposition.

We present here an investigation of transient photoconductivity of ZnO thin film grown by spray-pyrolysis as a function of an oxidant and inert atmospheres as well as in vacuum conditions in two different scenarios of illumination: above and below bandgap. We employed a clean chemical route based on zinc acetate diluted in an aqueous solution. Our results, based on X-rays diffraction (XRD), room temperature optical absorbance and photoluminescence measurements, show the presence of Urbach tail due to the presence of defects [14, 15]. A discussion based on photodesorption process explains that the presence of such defects allows the photoconductivity below bandgap excitation with an increased decay time in inert atmosphere comparable to the excitation above bandgap in vacuum.

2. Materials and Methods

2.1. Thin Film Growth. Spray pyrolysis technique was employed to grow a ZnO thin film on top of soda-lime glass substrate. The substrate area is as large as $18 \times 18\,\text{mm}^2$. The growth process is based on the pulverization of an aqueous solution containing 0.01 M zinc acetate dihydrate ($Zn(CH_3COO)_2 \cdot 2H_2O$) in distilled water. The flow rate of solution during deposition was kept constant at 0.5 ml/min while compressed air at 1 bar was used as carrier gas. The growth process was conducted in several spraying cycles starting at 300°C. During the deposition, the temperature of substrate drops and the cycle stops when the temperature is 220°C. Then, the cycle restarts when the substrate recovers the temperature of 300°C. A sketch of apparatus is depicted in Figure 1(a).

The chemical reaction responsible to form ZnO is considered a two-step process [16, 17], with prior dehydration of precursor followed by decomposition and oxidation of acetate molecule as follows:

$$\begin{aligned} Zn(CH_3COO)_2 \cdot 2H_2O &\rightarrow Zn(CH_3COO)_2 + 2H_2O \\ Zn(CH_3COO)_2 + 4O_2 &\rightarrow ZnO + 4CO_2 + 3H_2O \end{aligned} \quad (1)$$

The deposition process takes approximately 1.5 hours for a film thickness around 530 nm.

2.2. Characterization. Structural and morphological characterizations were performed by X-ray diffraction (XRD) measurements using a *Shimadzu* diffractometer *XRD-6100* (Cu-K_α at $\lambda = 1.5406$ Å) and a JEOL 5800 LV microscope for the scanning electron microscopy (SEM) of surface. Optical absorbance measurements were accomplished at room temperature using an *Agilent* UV-VIS-NIR Cary 5000 spectrophotometer in the range of 200–1100 nm. Photoluminescence measurements (PL) were carried out between 12 and 300 K by exciting the samples with the 325 nm line of a He-Cd laser. Indium was used as electrical contact distant 5 mm. A 10 V constant voltage was applied, and the electrical current was monitored as a function of time during the photoconductivity measurements. For light illumination, the lines 325 nm and 442 nm of HeCd laser (Kimmon-Koha) in a constant incident power of 10 mW were employed. The photoconductivity measurements were carried in free (air) atmosphere with relative humidity of ~17%.

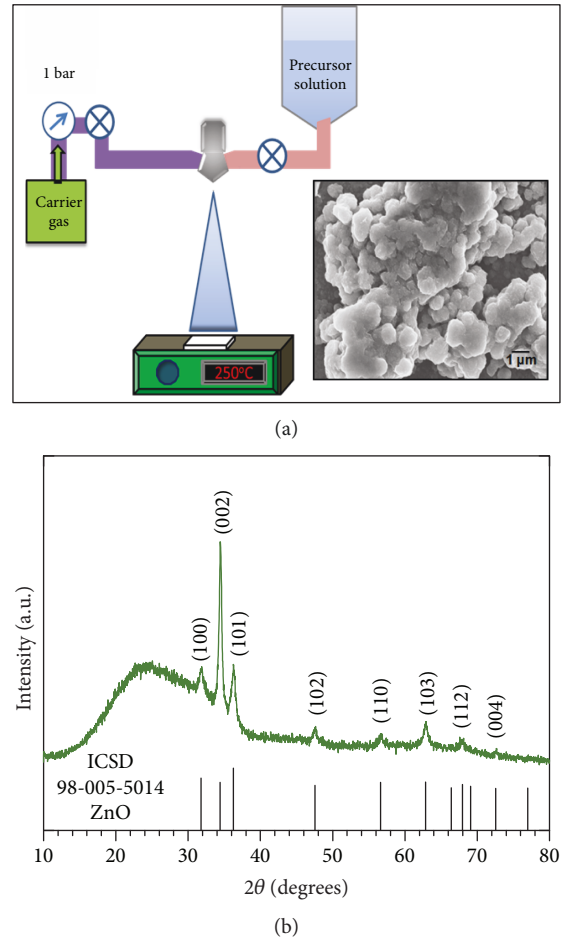

Figure 1: (a) The homemade spray-pyrolysis apparatus employs compressed air as carrier gas and an aqueous solution containing zinc acetate as precursor. The pulverization allows large area film growth, and the inset illustrates a SEM image. (b) XRD data show polycrystalline film with c-axis preferential direction for ZnO as compared to ICSD pattern.

3. Results and Discussion

The inset of Figure 1(a) exhibits a representative SEM image which shows grain formation pattern with submicron size. The wurtzite crystal structure is confirmed by XRD data for ZnO film in Figure 1(b) as compared to the pattern ICSD 98-005-5014. The broad band around $2\theta \sim 25^\circ$ is related to the amorphous glass substrate. The as-grown ZnO film

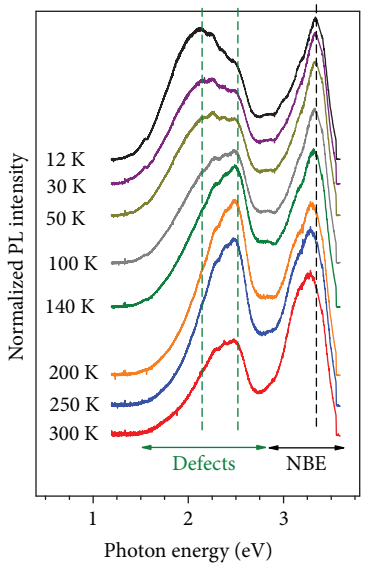

Figure 2: Temperature-dependent photoluminescence emission of ZnO thin film.

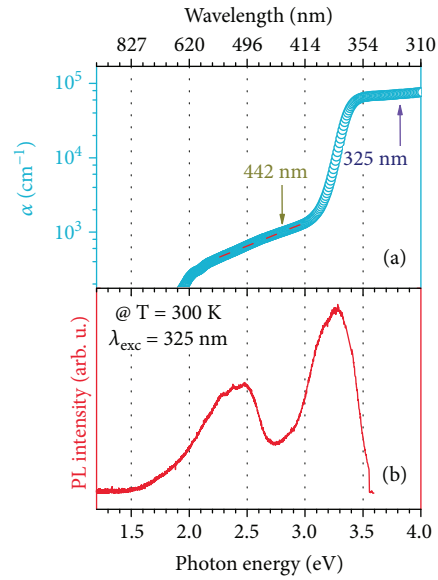

Figure 3: (a) The optical absorption coefficient of ZnO exhibits the strong absorption due to the direct bandgap in the UV range and the Urbach tail in the visible range. Our experiment employs both spectral regions as probe for photoconductivity measurements. (b) Photoluminescence spectrum at 300 K shows emission due to NBE at 3.3 eV and a broad band in the visible range related to defects.

presents a preferential orientation at (002) direction, which is recurrent in the literature [18–20] and is related to the lowest surface free energy of this plane [21].

The crystallite size D is evaluated applying the Scherrer's equation [22] in the line broadening of (002) peak: $D = K\lambda/\beta \cos\theta$, where λ is the wavelength for the Cu-K_α radiation (1.5406 Å), K is an empirical constant (0.94), and β is the corrected full width at half maximum (FWHM) in radians, which resulted $D = 13$ nm for as-grown ZnO thin film.

Temperature-dependent photoluminescence spectra are exhibited in Figure 2. Two broad bands are clearly distinguished. In the ultraviolet optical range (>2.8 eV), the emission centered at 3.35 eV is attributed to the near band edge (NBE). It is notable that it is broadening with full width at half maximum (FWHM) around 0.41 eV which indicates a disordered system where the NBE emission is in fact the convolution of several emissions related to free and bound excitons as well as conduction to acceptor levels [16, 20]. Additionally, the peak position presents a red shift as temperature increases. In addition, the broad emission in the visible optical range presents two emissions, one around 2 eV, stronger at low temperatures, and other around 2.5 eV, which dominates the room temperature emission. This optical band is known as yellow-green band and is related to crystalline defects like vacancies and interstitial sites which nature is still an interesting and controversial topic in the literature despite emission at 2.5 eV that is attributed to the recombination from oxygen vacancy levels to the valence band [20].

The optical absorption coefficient α is extracted from the absorbance measurements considering $\alpha = A/d$, where A is the measured absorbance corrected with substrate and d is the film thickness. Figure 3(a) shows the increase of absorption as the photon energy increases up to the bandgap. The absorption edge in the range of 355–415 nm corresponds to the direct bandgap of ZnO films. The optical energy bandgap can be obtained through the application of the Tauc's relation for direct allowed optical transition in a plot of $(\alpha h\nu)^2$ versus $h\nu$ (not shown here), and in this case, it was found a value of $E_g = 3.16$ eV [16, 19, 23]. Above bandgap, $\alpha \sim 10^5$ cm^{-1} is a standard value for good optical absorbers.

Below 3.0 eV (~415 nm), the linear region observed in the exponential scale presents a lower absorption coefficient and it is attributed to defect-band absorption due to tail related to localized states near band edges. This behaviour is expressed by Urbach rule [14] as

$$\alpha = \alpha_0 \cdot \exp\left(\frac{h\nu}{E_U}\right), \tag{2}$$

where α_0 is the preexponential factor, $h\nu$ is the incident photon energy, and E_U is the Urbach energy associated to the band tail width or energy of disorder. From data presented in Figure 3(a), the equation fitting gives us $\alpha_0 = (17.5 \pm 0.1)$ cm^{-1} and $E_U = (697 \pm 3)$ meV. The literature reports vast values of Urbach energies from 60 meV to 1000 meV which is very dependent on the synthesis methods as well as the growth parameters used in each process [24].

The photoluminescence spectrum at room temperature in Figure 3(b) corroborates the discussed behaviour related to optical absorption. The optical excitation above bandgap mainly promotes electrons to the conduction band. The optical recombination from conduction to valence attributed to the near bandgap edge (NBE) is centered in 3.28 eV with the increase in the FWHM to 0.48 eV while the main contribution to defect-related optical band now is around 2.5 eV. The comparison between absorption and emission at room temperatures is an indicative that the excitation below bandgap energy will play with defect levels in the bandgap.

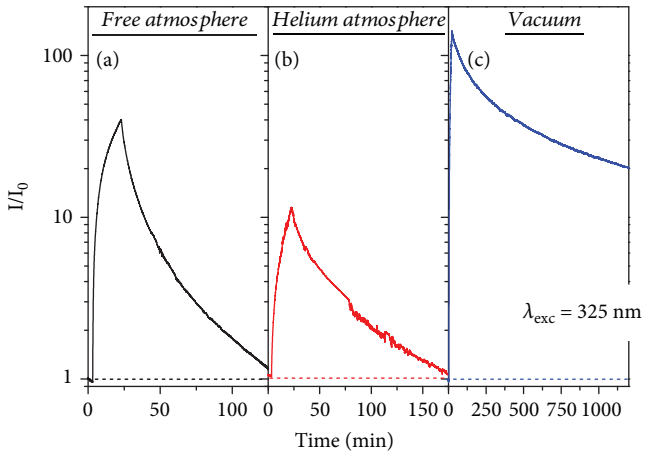

Figure 4: Transient photoconductivity of ZnO thin film obtained by spray-pyrolysis when the illumination is above the bandgap considering the conditions of (a) free (air) atmosphere, (b) helium (inert) atmosphere, and (c) under vacuum.

The influence of atmospheres on photoconductivity responses was investigated taking into account two scenarios: (i) a band to band optical absorption with $\lambda_{exc} = 325$ nm and (ii) defect-related absorption associated to Urbach tail with $\lambda_{exc} = 442$ nm. In both cases, the incident laser excitation was kept constant at 10 mW. Under these situations, the transient photoconductivity measurements were performed in a free atmosphere in a closed cryostat at room temperature as a chamber. For vacuum conditions, the chamber is evacuated and the vacuum level is kept constant at 10^{-4} mbar for the experiment. Finally, for inert atmosphere experiment, the chamber is filled up to 1 bar with high-purity helium gas. The sample is illuminated during 20 min for all cases, and the photoconductivity is considered the response to this illumination up to a maximum increase of electrical current followed by a period after the illumination is interrupted.

Figure 4 shows the transient photoconductivity when the optical excitation is above bandgap ($\lambda = 325$ nm). The increase of electrical current is observed for all conditions, but any saturation in the conductivity up to 20 min is not observed. Additionally, when the illumination is interrupted, the recoveries are not immediate. The influence of atmospheres in the response and in the rise and recovery times is notable.

Under free atmospheric condition, the electrical current increases around 50 times (Figure 4(a)). Actually, the recovery to the initial state has different contributions due to processes like recombination between electrons from the conduction band to holes in the valence band, which is in the range between 10^{-14} and 10^{3} seconds [25], trapped photocarriers in defect-related localized states which are released back to conduction/valence bands [6, 7], and adsorption/desorption kinetics of atmosphere specimens which react with the solid surface [26]. Therefore, the transient decay is an average of these processes which can be modelled as

$$\frac{I}{I_0} = \sum_{1}^{3} A_n * \exp\left[-\frac{t}{\tau_n}\right], \quad (3)$$

where A_n is a fitting constant and τ_n is the time constant related to each process. In order to achieve a coherent interpretation of fitting parameters, we discuss the average $<\tau>$ as the arithmetic average of τ_n.

Accordingly, the main difference between atmospheres is the chemical reactivity. In the case of free atmosphere, we attribute the main reactivity to the presence of oxygen. As can be noted in Figures 4(a) and 4(b), the time recovery for air atmosphere is quite fast as compared to inert atmosphere of helium. An important parameter to be considered is the response R defined as $R = |I_{max} - I_0|/I_0$, where I_0 is the electrical current in dark before illumination. Despite the photoconductivity response in helium atmosphere being around a quarter (R~10) as compared to air atmosphere (R~40), the necessary time to recovery initial state is almost twice (τ~36 min) as compared to free atmosphere (τ~19 min). In vacuum (Figure 4(c)), the scenario is drastic: the response $R = 140$ while the recovery time takes more than 500 min and the conductivity does not return to the initial state. This is a characteristic of persistent photoconductivity which is discussed further.

In the case of free atmosphere (air), the main molecules present are oxygen, nitrogen, and water vapour molecules. The nitrogen molecules are chemically inactive due to the necessary energy to break its triple bonds [27]. Actually, the presence of water plays a fundamental role as the chemisorption of water molecules results in hydroxyl which acts as donor due to its lower electron affinity and ionization. But the relevance of water vapour molecules depends on the humidity levels (RH) in the air that can be classified like dry (RH < 20%) or wet (RH > 20%) as the ratio of these molecules is different [27]. If a single electronegative molecule such as oxygen approaches the semiconductor surface and its electron affinity χ_O is larger than the semiconductor work function W_S, then the molecule will capture an electron and become adsorbed on the surface. As a consequence, the molecule acts as an acceptor level and induces an upward band bending at the surface. However, similar considerations can be applied for an electropositive gas such as water vapour: the molecule will act as a donor level inducing a downward band bending at the surface [28]. In addition, ZnO is a typical intrinsic n-type semiconductor due to the presence of donor levels related to oxygen vacancies. Consequently, in the case of dry atmosphere and the n-type conductivity of ZnO, the adsorption of oxygen molecules on the semiconductor surface due to its electronegativity is more favourable. In fact, in a flatband picture associated to ZnO (Figure 5(a)) concerning oxygen presence, the adsorption of molecules as negatively charged ion is due to the capture of free electrons from conduction band. This is a cause of the higher resistance observed under free atmosphere compared to vacuum conditions which is characterized by the formation of a depletion layer L_D at the surface (Figure 5(b)). When the oxide is illuminated above bandgap, photogenerated holes move to the surface causing the discharge of negative adsorbed ions. As a consequence, these molecules can now be desorbed from the surface in a photodesorption process [29]. In air atmosphere, there is a constant flux of oxygen molecules

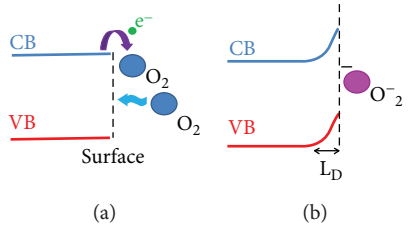

Figure 5: Oxygen adsorption process: (a) free electrons at the ZnO surface are captured by oxygen molecules and (b) as a consequence, an upward band bending is formed at the ZnO surface creating a depletion layer.

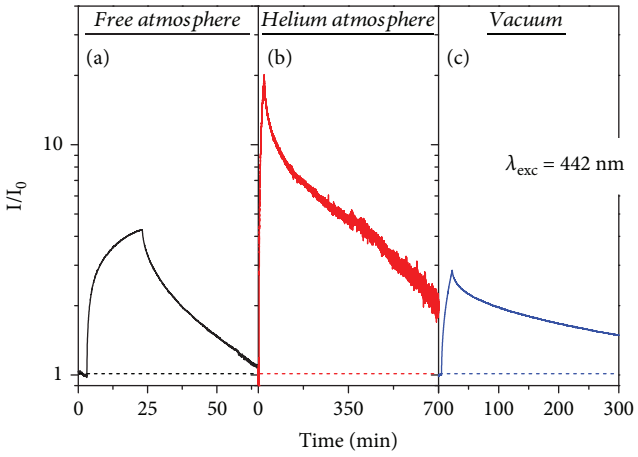

Figure 6: Transient photoconductivity of ZnO thin film obtained by spray-pyrolysis when the illumination is below the bandgap, in the region of Urbach tail, considering the conditions of free (air) atmosphere, helium (inert) atmosphere, and under vacuum.

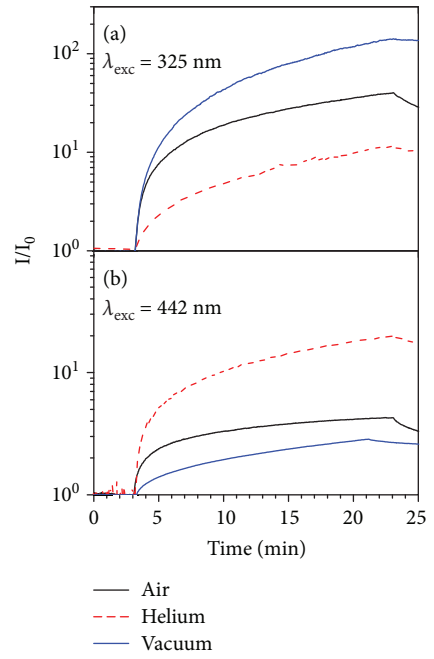

Figure 7: The raise of photoconductivity during 20 min light exposition (a) above bandgap and (b) below bandgap.

which contributes to shorter decay times as compared to other atmospheres. In an inert atmosphere and vacuum, the lack of oxygen molecules is responsible for larger decay times as observed. In contrast, the influence of persistent photoconductivity due to electron trapping in defect levels is enhanced for vacuum condition. As these traps avoid the recombination to the fundamental state, and there is no other relaxation process as under oxygen presence, the decay time increases one order of magnitude as observed in Figure 4(c).

In a perfect semiconductor, photoconductivity excited below bandgap would be negligible. In contrast, due to the presence of defects or impurities, localized states are formed in the bandgap region. Some of these states can be populated by electrons, dislocating the Fermi level, and in some cases give a nonintentional intrinsic conductive behavior. The loss of stoichiometry is a well-known mechanism which creates defects in oxide-based materials and is responsible for the n-type conductivity in ZnO and TiO_2 while it makes CuO a p-type semiconductor [30–32]. Figure 6 shows the atmosphere-dependent photoconductivity when excitation is performed below bandgap of ZnO. The photoresponse under air atmosphere (Figure 6(a)) and vacuum (Figure 6(c)) is strongly decreased to 4 and 0.7, respectively, as discussed above. The possibility of a photoconductive below bandgap is justified by the presence of defect-related absorption present due to Urbach tail shown in Figure 3(a). In order to influence the conductivity, such absorptions should be attributed from defects near valence bands which promote electrons to the conduction band. As compared to excitation above bandgap, an increase of decay times is also observed for both cases as well as in helium atmosphere. In opposite of excitation above bandgap, the excitation now is from localized states near valence band and consequently the fundamental state is not in the valence band, changing the previously observed dynamics. Similarly, the role of adsorbed molecules and photodesorption is relevant. While the effect of charging adsorbed molecules is dependent of the quantity of oxygen molecules in the atmosphere, now the efficiency of photodesorption is decreased as in the band bending no free holes are available in valence band to promote the discharge of negatively charged oxygen molecules on surface. This can explain the increase of time decays in the Urbach tail condition. As expected, the persistent photoconductivity in vacuum conditions is still present due to its inherent nature associated to traps close to conduction band. The decrease of photodesorption process is corroborated in the inert atmosphere (Figure 6(b)), which presents the highest photoresponse (R~20) when the excitation is in the Urbach tail optical range.

Figure 7 shows the transient increase of photoconductivity for different atmospheres and excitations. It is interesting to point out that thermal excitation can form oxygen vacancies in the surface of ZnO, which is a reversible process. Analogously, under illumination, the charged oxygen ions can recombine with weakly bound surface oxygen to form O_2 in gaseous state and leave the solid. This

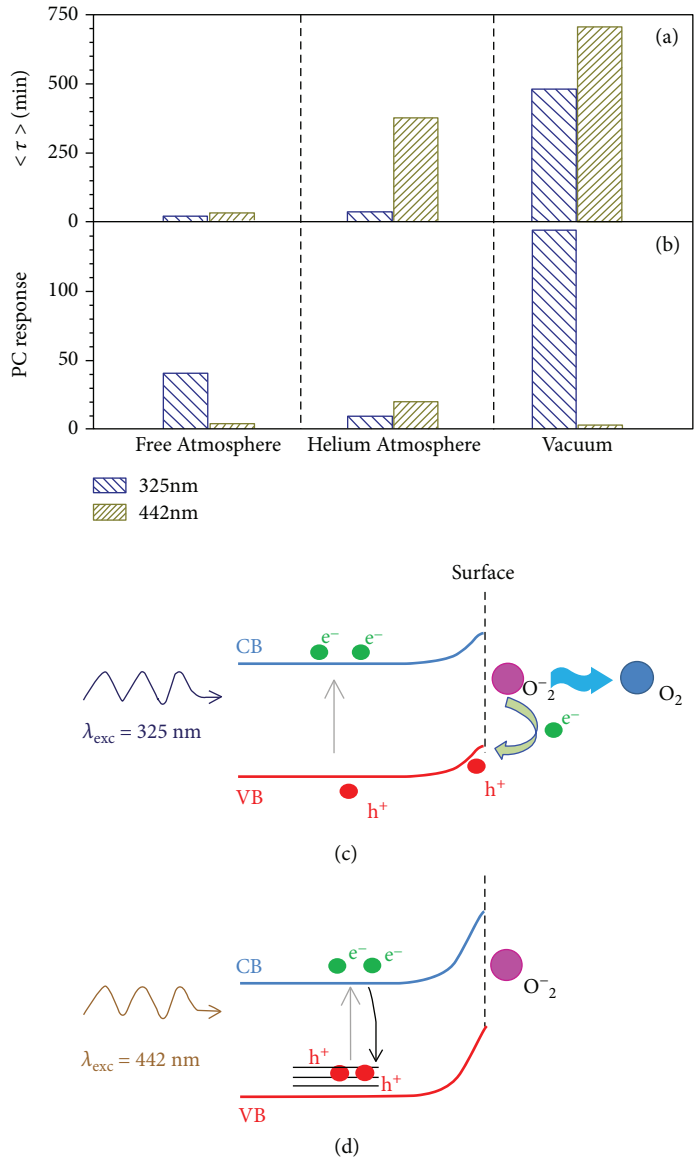

Figure 8: The comparative results between (a) time decays and (b) photoconductive responses in air, inert atmosphere and vacuum conditions with light excitation above and below ZnO bandgap. (c) In an air atmosphere, an oxygen photodesorption occurs when the excitation is above bandgap due to free hole concentration in valence band. (d) When the excitation is below bandgap, the oxygen photodesorption process is suppressed. The main effect of excitation in the Urbach tail is the decrease of photodesorption causing the increase of photoconductivity decay times.

effect is attributed to a solid-state reaction with oxygen molecules adsorbed on the surface of ZnO [29], which is similar to the observed for TiO_2 [33].

$$\mathrm{ZnO(s)} + h\nu \rightarrow \mathrm{ZnO}_{1-\delta} + \frac{\delta}{2}\mathrm{O_2(g)} \quad (4)$$

Consequently, the raises of photoconductivity have a similar slope in the first seconds in vacuum and air atmospheres when excited above bandgap (Figure 7(a)). The higher response in such cases is attributed to the effective removal of gaseous formation under vacuum followed by the presence of more specimens of O molecule in air, while under an inert atmosphere, the overpressure tends to balance the oxygen degas. As the overpressure condition is the same, the response and raise keep the behavior quite similar under illumination in the Urbach tail (Figure 7(b)). As the main reason for the photodesorption is the presence of free holes near surface, the illumination below bandgap relieves the desorption of oxygen in gaseous form as indicated by the behavior of photoconductivity in Figure 7(b) as compared to Figure 7(a) for vacuum and air atmosphere.

Figure 8 summarizes our results: (i) for excitation above bandgap, the photoconductivity time decays $<\tau>$ (Figure 8(a)) are longer when the presence of oxygen or an overpressure in atmosphere is decreased while the photoresponse increases in the absence of oxygen (Figure 8(b)). This occurs due to effect of discharging adsorbed ions due to

presence of free holes near surface (Figure 8(c)); (ii) when the excitation is below bandgap, the photoresponse decreases significantly but it is still present in disordered systems with Urbach tail. In such case, the excitation does not promote electrons from valence band and the photoconductivity is due to the promotion of electrons present to the defect-related levels near valence band as schematized in Figure 8(d). Consequently, the photodesorption of adsorbed molecules is absent and the time decays strongly increase for excitations in the Urbach tail.

4. Conclusions

The growth of zinc oxide thin films by spray-pyrolysis represents an alternative to large-scale and industrial production plant. As-grown ZnO thin films have the wurtzite structure in polycrystalline form with (002) preferential direction when grown on glass. Optical absorbance measurements show the presence of electronic defects in the bandgap by absorption in the Urbach tail with an energy around 700 meV. The photoconductivity is explored in two regimes of light excitation, above and below ZnO bandgap, in oxidant and inert atmospheres as well as in vacuum conditions. The increase of photoconductivity time decays when excited below bandgap is attributed to the mitigation of oxygen photodesorption. Our results indicate a suitable mechanism to achieve longtime photoconductivity for related applications.

Data Availability

The data used to support the findings of this study are available from the corresponding author upon request.

Conflicts of Interest

The authors declare that they have no conflicts of interest.

Acknowledgments

This work was supported by FAPESP (grant 2016/10973-4). Fellowships from CAPES and CNPq are acknowledged. The authors thank N. Zanardi for XRD and Prof. A.D. Rodrigues for UV-VIS absorption measurements.

References

[1] H. Yu, J. Wang, Y. Yan et al., "ZnO thin films produced by the RF magnetron sputtering," in *Proceedings of 2011 International Conference on Electronic & Mechanical Engineering and Information Technology*, pp. 2486–2489, Harbin, China, 2011, IEEE.

[2] J. Zhao, L. Hu, Z. Wang et al., "Growth and photoluminescence of ZnO thin films on Si(1 1 1) by PLD in oxygen adequate ambient," *Vacuum*, vol. 81, no. 9, pp. 1035–1039, 2007.

[3] V. Craciun, J. Elders, J. G. E. Gardeniers, and I. W. Boyd, "Characteristics of high quality ZnO thin films deposited by pulsed laser deposition," *Applied Physics Letters*, vol. 65, no. 23, pp. 2963–2965, 1994.

[4] Y. W. Heo, D. P. Norton, and S. J. Pearton, "Origin of green luminescence in ZnO thin film grown by molecular-beam epitaxy," *Journal of Applied Physics*, vol. 98, no. 7, article 073502, 2005.

[5] R. Ayouchi, D. Leinen, F. Martın, M. Gabas, E. Dalchiele, and J. R. Ramos-Barrado, "Preparation and characterization of transparent ZnO thin films obtained by spray pyrolysis," *Thin Solid Films*, vol. 426, no. 1-2, pp. 68–77, 2003.

[6] S. de Castro, D. A. W. Soares, M. L. Peres, P. H. O. Rappl, and E. Abramof, "Room temperature persistent photoconductivity in *p*-PbTe and *p*-PbTe:BaF_2," *Applied Physics Letters*, vol. 105, no. 16, article 162105, 2014.

[7] L. M. B. Vargas, S. de Castro, M. L. Peres, M. P. F. de Godoy, and D. A. W. Soares, "Tuning positive and negative photoconductivity in $Zn_{1-x}Cd_xO$ films," *Journal of Alloys and Compounds*, vol. 749, pp. 734–740, 2018.

[8] L. F. da Silva, J. C. M'Peko, A. C. Catto et al., "UV-enhanced ozone gas sensing response of ZnO-SnO_2 heterojunctions at room temperature," *Sensors and Actuators B: Chemical*, vol. 240, pp. 573–579, 2017.

[9] G. H. Munshi, A. M. Ibrahim, and L. M. Al-Harbi, "Inspired preparation of zinc oxide nanocatalyst and the photocatalytic activity in the treatment of methyl orange dye and paraquat herbicide," *International Journal of Photoenergy*, vol. 2018, Article ID 5094741, 7 pages, 2018.

[10] M. C. Tarun, F. A. Selim, and M. D. McCluskey, "Persistent photoconductivity in strontium titanate," *Physical Review Letters*, vol. 111, no. 18, article 187403, 2013.

[11] P. Zhang, G. Pan, B. Zhang, J. Zhen, and Y. Sun, "High sensitivity ethanol gas sensor based on Sn - doped ZnO under visible light irradiation at low temperature," *Materials Research*, vol. 17, no. 4, pp. 817–822, 2014.

[12] H. Akazawa and H. Shinojima, "Energy dissipation channels affecting photoluminescence from resonantly excited Er^{3+} ions doped in epitaxial ZnO host films," *Journal of Applied Physics*, vol. 117, no. 15, article 155303, 2015.

[13] S. Rahmane, M. A. Djouadi, M. S. Aida, N. Barreau, B. Abdallah, and N. Hadj Zoubir, "Power and pressure effects upon magnetron sputtered aluminum doped ZnO films properties," *Thin Solid Films*, vol. 519, no. 1, pp. 5–10, 2010.

[14] F. Urbach, "The long-wavelength edge of photographic sensitivity and of the electronic absorption of solids," *Physics Review*, vol. 92, no. 5, p. 1324, 1953.

[15] Y. Caglar, S. Ilican, M. Caglar, and F. Yakuphanoglu, "Effects of In, Al and Sn dopants on the structural and optical properties of ZnO thin films," *Spectrochimica Acta Part A: Molecular and Biomolecular Spectroscopy*, vol. 67, no. 3-4, pp. 1113–1119, 2007.

[16] Y. J. Onofre, S. de Castro, and M. P. F. de Godoy, "Effect of traps localization in ZnO thin films by photoluminescence spectroscopy," *Materials Letters*, vol. 188, pp. 37–40, 2017.

[17] T. Fukui, S. Ohara, M. Naito, and K. Nogi, "Synthesis of NiO–YSZ composite particles for an electrode of solid oxide fuel cells by spray pyrolysis," *Powder Technology*, vol. 132, no. 1, pp. 52–56, 2003.

[18] M. B. Rahmani, S. H. Keshmiri, M. Shafiei et al., "Transition from *n*- to *p*-type of spray pyrolysis deposited Cu doped ZnO thin films for NO_2 sensing," *Sensor Letters*, vol. 7, no. 4, pp. 621–628, 2009.

[19] S. de Castro, S. L. dos Reis, A. D. Rodrigues, and M. P. F. de Godoy, "Defects-related optical properties of $Zn_{1-x}Cd_xO$ thin

films," *Materials Science and Engineering: B*, vol. 212, pp. 96–100, 2016.

[20] N. L. Tarwal, K. V. Gurav, T. Prem Kumar et al., "Structure, X-ray photoelectron spectroscopy and photoluminescence investigations of the spray deposited cobalt doped ZnO thin films," *Journal of Analytical and Applied Pyrolysis*, vol. 106, pp. 26–32, 2014.

[21] V. Khranovskyy, I. Tsiaoussis, L. Hultman, and R. Yakimova, "Selective homoepitaxial growth and luminescent properties of ZnO nanopillars," *Nanotechnology*, vol. 22, no. 18, article 185603, 2011.

[22] B. D. Cullity and S. R. Stock, *Elements of X-Ray Diffraction*, Prentice Hall, 2001.

[23] J. I. Pankove, *Optical Processes in Semiconductors*, Dover, 1975.

[24] O. Belahssen, H. Ben Temam, S. Lakel, B. Benhaoua, S. Benramache, and S. Gareh, "Effect of optical gap energy on the Urbach energy in the undoped ZnO thin films," *Optik - International Journal for Light and Electron Optics*, vol. 126, no. 15-16, pp. 1487–1490, 2015.

[25] R. H. Bube, *Photoconductivity of Solids*, John Wiley and Sons Inc., New York, NY, USA, 1969.

[26] J. M. Thomas and W. J. Thomas, *Principles and Practice of Heterogeneous Catalysis*, VCH, Weinheim, Germany, 1997.

[27] P. Shankar and J. B. Rayappan, "Gas sensing mechanism of metal oxides: the role of ambient atmosphere, type of semiconductor and gases-a review," *Science Letters*, vol. 4, p. 126, 2015.

[28] A. Many, Y. Goldstein, and N. B. Grover, *Semiconductor Surfaces*, North Holland Publishing Company, Amsterdam, Netherlands, 1971.

[29] Y. Takahashi, M. Kanamori, A. Kondoh, H. Minoura, and Y. Ohya, "Photoconductivity of ultrathin zinc oxide films," *Japanese Journal of Applied Physics*, vol. 33, 12A, Part 1, pp. 6611–6615, 1994.

[30] L. Liu, Z. Mei, A. Tang et al., "Oxygen vacancies: the origin of *n*-type conductivity in ZnO," *Physical Review B*, vol. 93, no. 23, 2016.

[31] A. Tombak, M. Benhaliliba, Y. S. Ocak, and T. Kiliçoglu, "The novel transparent sputtered p-type CuO thin films and Ag/p-CuO/n-Si Schottky diode applications," *Results in Physics*, vol. 5, pp. 314–321, 2015.

[32] M. Hübner, C. E. Simion, A. Tomescu-Stanoiu, S. Pokhrel, N. Bârsan, and U. Weimar, "Influence of humidity on CO sensing with p-type CuO thick film gas sensors," *Sensors and Actuators B: Chemical*, vol. 153, no. 2, pp. 347–353, 2011.

[33] R. Amade, P. Heitjans, S. Indris, M. Finger, A. Haeger, and D. Hesse, "Influence of gas atmosphere and temperature on the conductivity and the photoconductivity of a TiO_2 single crystal in the surface region," *Physical Chemistry Chemical Physics*, vol. 8, no. 6, pp. 777–782, 2006.